Supporting Information
The Apeli: An Affordable, Low-Emission and Fuel-Flexible Tier 4 Advanced Biomass Cookstove

Dennis Krüger*, Özge Mutlu

Dr.-Ing. Dennis Krüger

Deutsches Biomasseforschungszentrum gemeinnützige GmbH (DBFZ), Torgauer Straße 116, 04347 Leipzig, Germany

E-Mail: dennis.krueger@dbfz.de

Tel: +49-341-2434-759

ORCID: 0000-0001-7554-6591

Dr. Özge Mutlu

Deutsches Biomasseforschungszentrum gemeinnützige GmbH (DBFZ), Torgauer Straße 116, 04347 Leipzig, Germany

ORCID: 0000-0003-4341-7714

S1. Background Information

Togolese Republic is located in west Africa with a total area of 56,785 km² with capital of Lomé. The country shares borders with Burkina Faso in the north, Benin in the east and Ghana in the west. The human index of the country is 0.41, which normally varies between 0 - 1. The reported population of the country in 2020 is 8.2 million and urban population accounts 73.5% of total population [30, 31]. The climate in Togo shows fluctuations from south to north. In southern part, the temperatures range between 18 – 32 °C whereas in northern part between 18 – 38 °C. The country has a dry climate and characteristics of a tropical savanna. Rainfall in the south of the country comes in the form of two seasons; the first between April and July and the second between September and November [32]. Agriculture is the leading sector, which shares nearly 40 % of gross domestic product (GDP) and employs 70 % of the population. Coffee, cocoa, cassava, sorghum, corn, rice and cotton are some of the important agricultural products of the country. 80 % of the overall energy consumption is met by traditional sources, especially biomass and 30 % increase in wood consumption is expected by 2025 [32].

The village Dévémé, located 60 km north of capital Lomé is selected as "study field" with the recommendation of the Togolese project partners. The selected location does not have access to electricity. There is a fountain serving as water source in the village which is used for drinking, washing and cooking etc. During rainy seasons, the rainwater is collected and used as water source, especially for washing. The houses in the village are either in banco or in cement, covered with sheets or straw. A field survey was carried out with 40 households, mostly with women who are the main actors and focus group in cooking activities. The details of the field survey are not the focus of this study, yet the answers are important to understand the daily dynamics of the local community and provided a good basis in development of the stove for clean cooking. Briefly; the total population of the households is 127 including 69 females and 58 men. The average household population is 3.2, while the age average of the participants is 31 varying between 2 - 90 years old. The average years completed at school is 5.8 years. In the surveys, any of the households did not indicate a specific monthly wage as income. The interviewers reported that, it is difficult to make an estimation on the monthly income of the participants, considering that majority of the community lives on agriculture, mostly growing yam, cassava and corn. According to survey results, the cooking activity is carried out typically 2 - 3 times daily in the half of the households. The participants indicated that they have a separate outdoor kitchen

for cooking and women are responsible for cooking activity. The majority of the participants (70 %) indicated that the preparation of one meal in average takes 1 - 2 hours. The typical dishes cooked are mostly rice, tomato sauce, dough and corn-based paste. In the village, the households use traditional fire places (see Fig. S1) which is self-built from mud and/or brick. The participants were asked, if they replace their cookstove (traditional stove in this case) throughout the year and 37.1 % answered with "yes". The reasons for replacing the cookstove are not being appropriate for long-term use, not being fuel-flexible, the need for repair. The participants indicated that they use their traditional stove for multiple purposes such as for cooking meals, boiling water, preparation of bath water. According to participants, the major problem of the current traditional stove is the emissions followed by not being fuel-flexible or appropriate for long-term use, in addition to the need of longer cooking times and difficulty to clean it after using. During one of the visits in the village, some of the village residents were asked about their complaints when they are cooking and their responds are in line with the answers of the survey. They mentioned that due to the smoke they have pain in the eyes and feel tired during pregnancy. They also find it challenging to prepare food because the fire does not start quickly. The residents also mentioned that they were not aware of these hazardous effects during cooking.

Figure S1: Typical traditional stove used for cooking in the selected village Dévémé in Togo (photo taken by the authors)

S2. Geometry of the combustion chamber

The combustion chamber of the Apeli consists of two components. The cylindrical casing, which is made of a 73 x 110 mm can (Fig. S2 a), and a temperature-resistant bottom made of stainless steel (Fig. S2 b).

The casing has the secondary air openings, which are arranged in 4 rows of 15 holes each. The successive rows are twisted against each other by 12 degrees and have a distance of 10 mm. The distance between the upper edge of the combustion chamber and the center of the secondary air openings from the first row is 20 mm. The holes have a diameter of approx. 3.3 mm.

The bottom of the burning chamber is made of 1 mm thick stainless steel (1.4301) and has 15 holes. These are arranged in two circular rows (8 and 6 holes) and a centered hole. The distance of the rows from the center point is 14 mm and 25 mm. For the experiments, two different bottoms were used which differ in the hole diameters. For the pellet fuels (WP, BP and SP) the holes have a diameter of 3.3 mm. For palm kernel shells (PK) the hole diameter used is 6 mm.
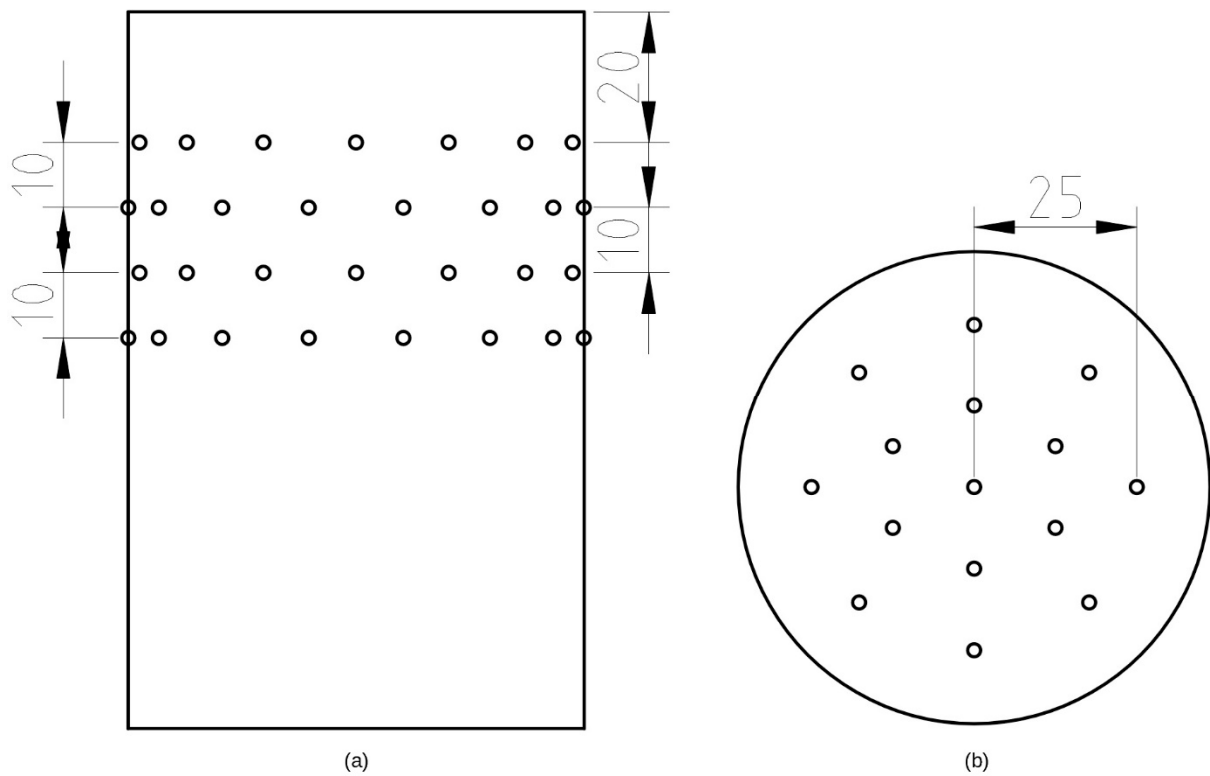

Figure S2: Geometry of the combustion chamber and openings for primary and secondary air; (a) 73 x 110 mm can based combustion chamber casing – side view; (b) bottom of the combustion chamber – top view; positions of the entry holes for primary (b) and secondary air (a) is given by the circular marks in the drawing
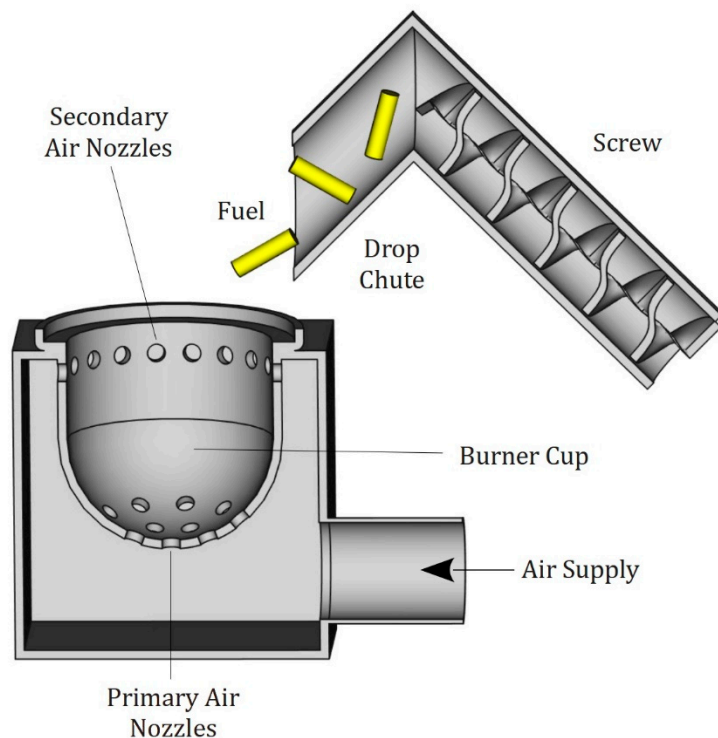
S3. Model for the combustion process used

Figure S3: 3D-Schematic of pellet stove type using a burner cup and fuel dropping system

Modern biomass furnaces for domestic heating are available in various structural designs for the combustion of biomass. The most important design types are grate firing, underfeed firing and firing with fuel dropping into a burner cup. For the development of the Apeli stove, the last-mentioned process was used as a technical starting point. This design type is mostly used in modern small-scale pellet boiler and stoves. An example for that is shown in Fig. S3. The main principle is based on the use of a small burner cup in which primary air is blown in from below for the gasification and pyrolysis of the fuel. Fresh fuel is continuously fed in from above using a fuel dropping system. The burner cup mostly (depending on the producer) have just few openings for secondary air. So, it is typically not enough secondary air supplied for complete combustion. Additional air is supplied often within the combustion chamber, which is lined with fireclay. It usually results in long flames. This does not cause any problems for pellet boiler or stoves, since the combustion chamber geometry can be adapted to the flame length. For single room heating pellet stoves with vision panel, this effect is even desirable, so that the user is able to see the flame.

For using this process as a cookstove, the user must thereby provide a continuous supply of fuel and the flame length should be reduced as far as possible to avoid direct contact between the flames and the bottom of the cooking pot. The contact of flames with colder (water-bearing) objects like heat exchanger lead to major quenching and higher emission values [33]. For a TLUD type experimental cookstove test bed, it could be shown that the presence of a pot has negative impact for CO as well as particle emissions [34]. Efforts to implement this during the development of the Apeli stove led to the geometry of the combustion chamber shown in Fig. S2.

S4. Test bed for emission and efficiency measurements

The test bed consists of a fully enclosed hood which has an opening in the direction of the user. Within this hood the stove emissions were collected and forwarded to the flue gas system. Due to the small power class of the Apeli stove in addition with low CO and particle matter values measured during pretests, no further dilution of the collected flue gas is carried out. The duct diameter is 10 cm and corresponds to the minimal recommended diameter according the ISO 19867-1:2018 standard. A blower in combination with a damper generates a volumetric flow of approx. 0.9 m³/min and ensures a fully turbulent flow with Re > 10^4. Due to the small duct diameter and the geometry of the particle measuring probe, the sampling points for gas and particle measurement are separate. In order to comply with the prescribed hydraulic inlet distance of the respective measuring points, the distance between the measuring points is > 4 x D.

Flue Gas

> 4 x D   > 4 x D

Velocity measurement   Gas measurement   Particle measurement   Damper

Duct diameter
D = 10 cm
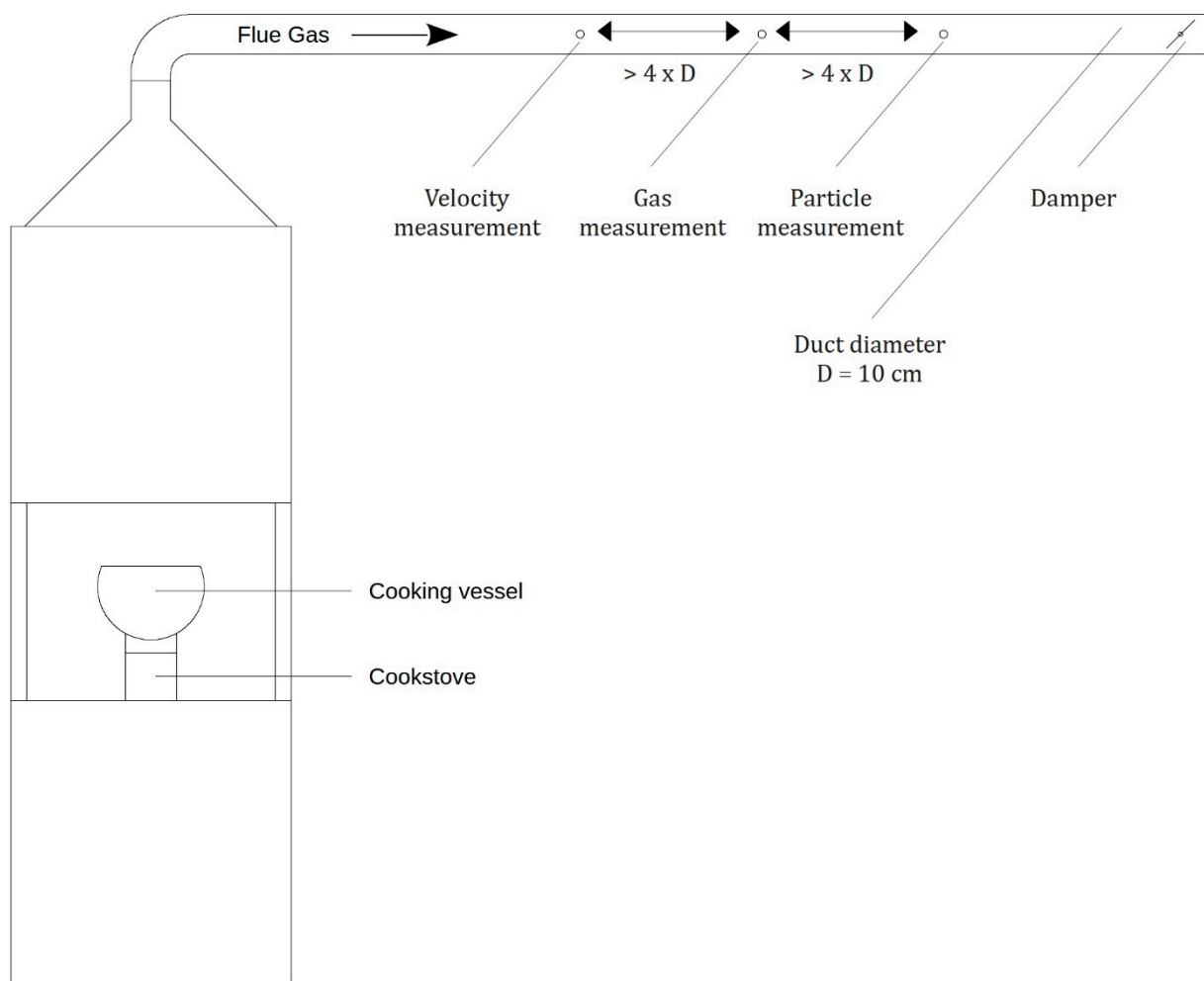
Cooking vessel

Cookstove

Figure S4: Schematic of the test bed used for measurements based on the ISO 19867-1:2018 standard.

S5. Detailed Data

Table S1: Detailed data of the experiments WP-H-L for modified ISO measurement based on ISO 19867-1:2018

Experiment		WP-H-L		
Number of tests		5		
Fuel		Feedstock	Wood	
		Form	Pellets	
		Moisture	7.5 %	
Metric		**Value**	**Unit**	**Sub-Tier**
Thermal efficiency with char credit	Mean	44.5	%	n.a.
	SD	0.4	%	
	90 % CI	**44.1** – 44.9	%	
Cooking Power	Mean	**1116**	W	n.a.
	SD	98	W	
PM2.5 per useful energy	Mean	15.2	mg/MJ$_d$	n.a.
	SD	2.7	mg/MJ$_d$	
	90 % CI	12.5 – **17.2**	mg/MJ$_d$	
CO per useful energy	Mean	0.208	g/MJ$_d$	n.a.
	SD	0.087	g/MJ$_d$	
	90 % CI	0.144 – **0.272**	g/MJ$_d$	
PM2.5 emission rate	Mean	1.0	mg/min	n.a.
	SD	0.1	mg/min	
	90 % CI	0.9 – **1.1**	mg/min	
CO emission rate	Mean	13.5	mg/min	n.a.
	SD	4.3	mg/min	
	90 % CI	10.3 – **16.7**	mg/min	

Table S2: Detailed data of the experiments WP-L-L for modified ISO measurement based on ISO 19867-1:2018

Experiment		WP-L-L		
Number of tests		5		
Fuel		Feedstock	Wood	
		Form	Pellets	
		Moisture	7.5 %	
Metric		**Value**	**Unit**	**Sub-Tier**
Thermal efficiency	Mean	38.4	%	n.a.
	SD	0.5	%	
	90 % CI	**38.0** – 38.8	%	
Cooking Power	Mean	**526**	W	n.a.
	SD	33	W	
PM2.5 per useful energy	Mean	43.5	mg/MJ$_d$	n.a.
	SD	2.2	mg/MJ$_d$	
	90 % CI	41.9 – **45.1**	mg/MJ$_d$	
CO per useful energy	Mean	1.058	g/MJ$_d$	n.a.
	SD	0.057	g/MJ$_d$	
	90 % CI	1.016 – **1.100**	g/MJ$_d$	
PM2.5 emission rate	Mean	1.4	mg/min	n.a.
	SD	0.1	mg/min	
	90 % CI	1.3 – **1.5**	mg/min	
CO emission rate	Mean	33.4	mg/min	n.a.
	SD	2.6	mg/min	
	90 % CI	31.5 – **35.3**	mg/min	

Table S3: Detailed data of the experiments WP-H-S for modified ISO measurement based on ISO 19867-1:2018

Experiment		WP-H-S		
Number of tests		3		
Fuel		Feedstock	Wood	
		Form	Pellets	
		Moisture	7.5 %	
Metric		**Value**	**Unit**	**Sub-Tier**
Thermal efficiency	Mean	42.9	%	
	SD	0.9	%	n.a.
	90 % CI	**42.1** – 43.8	%	
Cooking Power	Mean	**1094**	W	
	SD	50	W	n.a.
PM2.5 per useful energy	Mean	12.4	mg/MJ_d	
	SD	3.6	mg/MJ_d	n.a.
	90 % CI	9.0 – **15.8**	mg/MJ_d	
CO per useful energy	Mean	0.116	g/MJ_d	
	SD	0.019	g/MJ_d	n.a.
	90 % CI	0.097 – **0.135**	g/MJ_d	
PM2.5 emission rate	Mean	0.8	mg/min	
	SD	0.2	mg/min	n.a.
	90 % CI	0.6 – **1.0**	mg/min	
CO emission rate	Mean	7.6	mg/min	
	SD	1.0	mg/min	n.a.
	90 % CI	6.7 – **8.5**	mg/min	

Table S4: Detailed data of the experiments BP-H-S for modified ISO measurement based on ISO 19867-1:2018

Experiment		BP-H-S		
Number of tests		3		
Fuel		Feedstock	Bamboo	
		Form	Pellets	
		Moisture	7.7 %	
Metric		**Value**	**Unit**	**Sub-Tier**
Thermal efficiency	Mean	43.6	%	
	SD	0.1	%	n.a.
	90 % CI	**43.5** – 43.8	%	
Cooking Power	Mean	**1199**	W	
	SD	27	W	n.a.
PM2.5 per useful energy	Mean	29.2	mg/MJ_d	
	SD	1.8	mg/MJ_d	n.a.
	90 % CI	27.5 – **30.9**	mg/MJ_d	
CO per useful energy	Mean	0.131	g/MJ_d	
	SD	0.024	g/MJ_d	n.a.
	90 % CI	0.108 – **0.154**	g/MJ_d	
PM2.5 emission rate	Mean	2.1	mg/min	
	SD	0.1	mg/min	n.a.
	90 % CI	2.0 – **2.2**	mg/min	
CO emission rate	Mean	9.4	mg/min	
	SD	1.6	mg/min	n.a.
	90 % CI	7.9 – **10.9**	mg/min	

Table S5: Detailed data of the experiments SP-H-S for modified ISO measurement based on ISO 19867-1:2018

Experiment		SP-H-S		
Number of tests		3		
Fuel		Feedstock	Wheat straw	
		Form	Pellets	
		Moisture	8.3 %	
Metric		**Value**	**Unit**	**Sub-Tier**
Thermal efficiency	Mean	43.2	%	
	SD	0.5	%	n.a.
	90 % CI	**42.8** – 43.7	%	
Cooking Power	Mean	**884**	W	
	SD	35	W	n.a.
PM2.5 per useful energy	Mean	87.1	mg/MJ$_d$	
	SD	0.6	mg/MJ$_d$	n.a.
	90 % CI	86.5 – **87.7**	mg/MJ$_d$	
CO per useful energy	Mean	0.427	g/MJ$_d$	
	SD	0.065	g/MJ$_d$	n.a.
	90 % CI	0.365 – **0.489**	g/MJ$_d$	
PM2.5 emission rate	Mean	4.6	mg/min	
	SD	0.2	mg/min	n.a.
	90 % CI	4.5 – **4.8**	mg/min	
CO emission rate	Mean	22.5	mg/min	
	SD	9.9	mg/min	n.a.
	90 % CI	13.1 – **31.9**	mg/min	

Table S6: Detailed data of the experiments PK-H-S for modified ISO measurement based on ISO 19867-1:2018

Experiment		PK-H-S		
Number of tests		3		
Fuel		Feedstock	Palm kernel shells	
		Form	Shells	
		Moisture	11.1 %	
Metric		**Value**	**Unit**	**Sub-Tier**
Thermal efficiency	Mean	44.2	%	
	SD	0.2	%	n.a.
	90 % CI	**44.0** – 44.4	%	
Cooking Power	Mean	**1194**	W	
	SD	21	W	n.a.
PM2.5 per useful energy	Mean	13.4	mg/MJ$_d$	
	SD	2.8	mg/MJ$_d$	n.a.
	90 % CI	10.7 – **15.1**	mg/MJ$_d$	
CO per useful energy	Mean	0.200	g/MJ$_d$	
	SD	0.009	g/MJ$_d$	n.a.
	90 % CI	0.191 – **0.209**	g/MJ$_d$	
PM2.5 emission rate	Mean	1.0	mg/min	
	SD	0.2	mg/min	n.a.
	90 % CI	0.8 – **1.1**	mg/min	
CO emission rate	Mean	14.3	mg/min	
	SD	0.8	mg/min	n.a.
	90 % CI	13.5 – **15.1**	mg/min	

S6. Discussion regarding temporal linkage of water temperature and water mass measurement to calculate the useful energy delivered

For this study, both measurements with a longer burnout time (WP-H-L – ending after 35 min) and measurements finished directly at the end of the fuel burning period (WP-H-S – ending approx. after 31.5 min) were carried out. It was found that the efficiency values with longer burnout time (η_3) are higher than those which are terminated directly after the fuel burning period (η_1). This means that efficiency must be higher in the phase after the end of the fuel burning period (approx. 3.5 min) to raise the value. Using the mean thermal efficiency values (Table S1 an S3) and formula S1 to estimate the thermal efficiency of the burnout phase within the last 3.5 minutes (η_2) leads to the result shown in the table S7.

$$\eta_2 = \frac{35 \cdot \eta_3 - 31.5 \cdot \eta_1}{3.5} \qquad \text{Formula S1}$$

Table S7: Estimation of the thermal efficiency for burnout phase η_2 using the mean thermal efficiency values measured (η_3 - WP-H-L; η_1 - WP-H-S)

η_3 (%)	η_1 (%)	η_2 (%)
44.5	42.9	58.9

Accordingly, the estimated thermal efficiency should be 58.9 % for the burnout phase. This means that the efficiency during burnout phase must be clearly higher than during normal operation of the stove.

During stove development, temperature measurements of the hot gas jet were taken. The measuring point was located approx. 1 cm below the bottom of the pot. It was found that the temperature fluctuated due to fuel feeding approx. between 600 and 900 °C in normal operation with WP. During the burnout phase, it dropped rapidly to below 250 °C. With regard to the significantly lower exergy of the gas flow during burnout, it should be very unlikely to achieve same or even higher efficiency in this phase compared to normal operation from the authors' point of view.

The authors assume that the reason for this strange behavior can be found in formula 4 (Useful energy delivered calculation) of the ISO 19867-1:2018 standard and would like to formulate the following hypothesis: For the calculation of the delivered energy the "highest temperature attained of the water in the cooking vessel" and the difference in water mass ($G_1 - G_2$) are used. Both values are collected at different times; the highest temperature typically during normal operation and the difference in water mass at the end of the experiment. The waiting time after the fuel burning period allows further water to evaporate due to the high vapor pressure using the sensible heat of the water and the pot without the need for further heat from the stove. The amount of energy used by the water to evaporate during waiting time and thereby lower the water temperature from the maximum temperature to the temperature at the end of the test (which is not relevant according to the standard) is thus captured twice within the calculation; for heating-up the water from the temperature measured at the end of the experiment to the maximum temperature and for evaporating lowering the temperature from the maximum to the temperature at the end of experiment.

Table S8 shows the calculated values for the thermal efficiency using the highest measured water temperature according to the ISO 19867-1:2018 standard (η_{ISO}) and the measured water temperature at the end of the experiment (η_{End}).

Table S8: Comparison of thermal efficiencies using different water temperatures as input parameters for the calculation; η_{ISO} – using of the highest measured water temperature according the ISO 19867-1:2018 standard; η_{End} – using of the measured water temperature at the end of the experiment

	η_{ISO} (%)			η_{End} (%)		
	Mean	90 % CI	Mean – 90 % CI	Mean	90 % CI	Mean – 90 % CI
WP-H-L	44.45	0.33	44.12	42.73	0.11	42.62
WP-H-S	42.90	0.84	42.06	42.50	0.43	42.07

The results show that the efficiency at termination immediately after the end of fuel burning period (WP-H-S) is practically identical for both types of calculation (42.06 % vs. 42.07 %). In this case, the water temperature at the end of the test is very close to the maximum temperature measured and there is no time for additional water evaporation. For the case with waiting time based on the standard (WP-H-L) the difference is with 1.5 % significantly higher (44.12 % vs. 42.62 %). The difference of the calculated thermal efficiency between both measurements is with 0.55 % (42.62 % – 42.07 %) smaller using the temperature at the end than 2.06 % (44.12 % - 42.06 %) using the highest temperature.

Due to this behavior, the authors assume that the calculation of the useful delivered energy according to the ISO 19867-1:2018 standard leads generally to increased calculated efficiency values, which do probably not exist in practice. In addition, this leads also to lower emission factors and rates.

For this reason, the authors propose to examine this part of the standard and use both the water temperature as well as the water mass at the end of the experiment as the basis for calculating the useful delivered energy.

S7. Discussion regarding including of the thermal mass of the pot to calculate the useful energy delivered

According to the ISO 19867-1:2018 standard, the heat balance for calculating the thermal efficiency using formula 4 (Useful energy delivered calculation) only includes the water with the shares of heat capacity and evaporation. The thermal mass of the pot is neglected. From the point of view that appropriate tests should be carried out for each pot and that the user of the stove can just use the heat transported to the food within the pot, this is understandable. However, it makes it difficult to compare different literature sources, especially if very different pots are used in terms of mass and heat capacity.

The authors would like to show the impact on the calculated thermal efficiency using different pots. In this study, a heavy traditional pot made of aluminum (m = 1459 g; $c_{p,Alu}$ assumed with 0.896 kJ/(kg x K)) was used for the experiments. Champion et al. [10] used a pot which is lightweight in comparison to this and made of stainless steel (m = 815 g; $c_{p,SS}$ assumed with 0.477 kJ/(kg x K)). In addition to the higher mass of the aluminum pot used, aluminum also has a significantly higher heat capacity compared to stainless steel. To calculate the impact of using these different pots, an additional correction factor $Q_{1,cor.}$ was added to the delivered energy (ISO 19867-1:2018 - formula 4) from the experiments WP-H-L according to formula S2.

$$Q_{1,cor.} = (1.459 \cdot 0.896 - 0.815 \cdot 0.477) \cdot (T_2 - T_1) \qquad \text{Formula S2}$$

This correction factor is calculating the difference of the energy amount for the following hypothetical pot. A pot which has the shape of the pot from this study, but the mass and heat capacity of the pot used in the study of Champion et al. [10]. The calculated amount of energy would be available to the water in addition and also would be included into the calculation of the thermal efficiency. Table S9 shows the calculated values for the thermal efficiency using the original aluminum pot from this study (η_{Alu}) and the hypothetical pot with lower mass and heat capacity (η_{SS}). If the hypothetical pot would be used in this study, the calculated efficiency of the stove would be about 1.4 % higher (45.55 % - 44.12 %) for this measurement.

Table S9: Comparison of thermal efficiencies using the aluminum pot from this study (η_{Alu}) and a hypothetical pot with the same shape, but the mass and heat capacity of Champion et al. [10] (η_{SS})

WP-H-L	Mean	90 % CI	Mean – 90 % CI
η_{Alu}	44.45	0.33	44.12
η_{SS}	45.82	0.27	45.55

The authors are aware that, in addition to the mass and heat capacity of the pot, the geometry also has an influence on the result. However, integrating the pot into the heat balance would reduce the source of error in comparisons to geometry only. As a side effect, this change would also result in slightly lower calculated emission factors.

For this reason, the authors propose to examine this part of the standard and think about integrating the pot into the heat balance.